J. Phys. Chem. A **2000,** *104,* 2132−2137

Hydrogen Bonding in Methyl-Substituted Pyridine−Water Complexes: A Theoretical Study

Imre Pápai*

Institute of Isotope and Surface Chemistry, Chemical Research Centre, Spectroscopy Department,
H-1525 Budapest, P.O.B. 77, Hungary

Gábor Jancsó

KFKI Atomic Energy Research Institute, Physical Chemistry Department,
H-1525 Budapest, P.O.B. 49, Hungary

Received: November 17, 1999; In Final Form: January 3, 2000

Density functional theory (DFT) and second-order Møller−Plesset perturbation theory (MP2) are applied to determine the hydrogen bonding interaction energies in pyridine−water and in a set of methyl-substituted pyridine−water complexes. The results show that methyl substitution stabilizes the hydrogen bond and the degree of stabilization varies with the number and the position of methyl groups. It is demonstrated that the MP2 method yields more reliable relative stabilities for these complexes than does the applied DFT method, which does not take proper account of the dispersion interactions between water and the methyl groups in ortho positions. The comparison of the order of the computed association energies of methyl-substituted pyridine−water complexes with the experimentally observed sequence of the ease of miscibility of these molecules with water shows that there is no simple relationship between the miscibility behavior and the strength of hydrogen bond formed between water and methyl derivatives of pyridine.

I. Introduction

Reentrant phase transitions have long been of interest from both experimental and theoretical points of view.[1] Binary liquid mixtures that show a closed-loop phase diagram are a simple and elegant example of the systems exhibiting this phenomenon. In these liquid mixtures, the region above and below the loop represents the completely miscible reentrant phases, and the region within the loop refers to the partially miscible phase. In other words, these mixtures unmix both below an upper critical solution temperature and upon heating above a lower critical solution temperature. Reentrant phases are a direct consequence of the interplay between energy and entropy as that interplay is expressed in the interactions and motions of the molecules that make up the mixture.[1] By varying the delicate balance between like and unlike molecule interactions in the mixture, e.g., by adding a third component, the immiscibility loop can be made to shrink and disappear.

The liquid mixtures of various methyl-substituted pyridines with water, which have been extensively studied experimentally,[2−9] represent a very interesting model system from the theoretical point of view, too. By changing the position and/or the number of methyl groups on the pyridine ring one can drastically change the mixing properties of these compounds with water. For example, pyridine (Py) and different methylpyridines (MPy) are completely miscible with water, whereas dimethylpyridine(DMPy)−water systems display closed-loop miscibility curves.[2] It is remarkable that although 2-methylpyridine (2-MPy) and 3-methylpyridine (3-MPy) are completely miscible in all proportions at all temperatures with water, they are only partially miscible with heavy water.[3] On the basis of the results of the solubility studies and investigations of thermodynamic properties,[2,3,10] the methyl-substituted pyridines (msPy) can be arranged in order of ease of solution in water as follows: Py $\gg$ 4-MPy $>$ 2-MPy $>$ 3-MPy $\gg$ 2,6-DMPy $>$ 3,5-DMPy.

Various models[11−17] have been proposed to explain the reentrant miscibility in aqueous solutions and to rationalize the sensitivity of the shape of the closed-loop phase diagrams to the structural details of the interacting molecules. In these models a particularly important parameter is the strength of the hydrogen bond that forms between unlike molecules. A recently proposed model[17] predicts the extension of the immiscibility gap as the hydrogen-bonding strength increases whereas, by contrast, other models[12−16] predict its shrinkage when going from weaker to stronger hydrogen bonds.

In the present work, we explore the influence of methyl substitution in the pyridine ring on the strength of the hydrogen bond formed in the pyridine−water association. To this end, we carried out density functional theory (DFT) and second-order Møller−Plesset perturbation theory (MP2) calculations for the pyridine−water (Py−W) and for a series of methyl-substituted pyridine−water (msPy−W) 1:1 complexes, where the number and the position of the methyl groups were varied (see Figure 1).

Several recent works indicate that DFT can yield reasonable energetics and structural properties for the classical lone-pair ···H−O type (lp···H−O) hydrogen bonded complexes provided that the exchange-correlation functional and the orbital basis sets are properly chosen (for review works in this field we refer to refs 18 and 19; for more recent applications, see refs 20−24). Some of our investigated structures, however, involved interactions where dispersion forces were expected to be not negligible compared to electrostatic and induction forces. Due to the failure of currently available approximate exchange-correlation functionals to describe long-range dispersion forces,[25,26] the energies of these types of interactions are considerably

10.1021/jp994094e CCC: $19.00

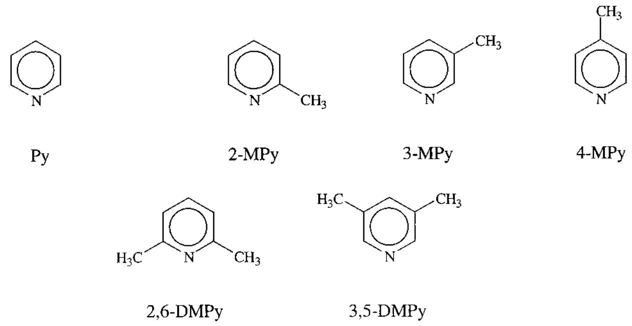

Figure 1. Investigated methyl-substituted pyridine molecules.

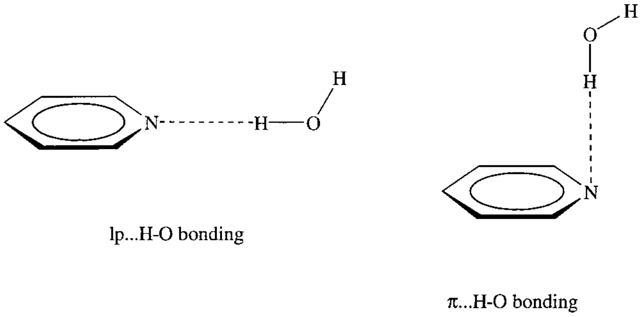

Figure 2. The lp···H−O and π···H−O interactions in Py−W.

underestimated.[21] Therefore, the interaction energies of all our investigated complexes were determined by means of MP2 calculations as well.

The main goals of our study were to determine the relative stability of various msPy−W complexes, establish a trend in the series, and compare it to the experimental miscibility properties.

II. Method and Computational Details

Two types of interaction between pyridine derivatives and water were considered in the present work (Figure 2). One of them corresponds to the global minimum of the msPy−W potential energy surfaces, where the interacting subunits are linked via nearly linear lp···H−O type hydrogen bonds. In the second structure, the water OH group is on top of the N atom of the pyridine ring and the interaction is described as π···H−O type hydrogen bonding.[27−31]

Both DFT and MP2 calculations were carried out using Dunning's augmented correlation consistent polarized valence double-ζ (aug-cc-pVDZ) basis set.[32,33] In the DFT calculations, the B3LYP exchange-correlation functional[34,35] was employed.

The geometry of the isolated monomers (W, Py, and msPy molecules) was fully optimized at the B3LYP/aug-cc-pVDZ level. The MP2 interaction energies were determined from single-point calculations carried out at the B3LYP equilibrium geometries. The geometry optimization for the π···H−O structures always converged into the global minimum, therefore, the effect of the methyl substitution on this type of interaction was investigated by deriving potential energy curves. In these calculations, the geometry of the monomers was always fixed at their B3LYP/aug-cc-pVDZ equilibrium geometries, the angle between the hydrogen bond and the pyridine ring was kept at 90°, the N···H−O angle was kept at 180° (see Figure 2), and only the intermolecular separation was varied. The harmonic vibrational frequencies of the investigated systems were computed at the B3LYP/aug-cc-pVDZ level too, and they served as data to estimate the zero point vibrational energies (ZPE). The basis set superposition error (BSSE) for the interaction energies was estimated using the counterpoise technique.[36]

TABLE 1: Selected Equilibrium Properties of Py and msPy Molecules Obtained from B3LYP/aug-cc-pVDZ Calculations[a]

	μ^b	$\bar{\alpha}^b$	Q_N	ΔPA^c
Py	2.28 [2.35, 2.22[d]]	9.58 [9.47]	−0.488	0.0 [0.0]
2-MPy	1.90 [2.20]	11.68 [11.69]	−0.501	4.5 [4.2]
3-MPy	2.55 [2.45]	11.63 [11.54]	−0.483	3.6 [3.3]
4-MPy	2.80 [2.68]	11.62 [12.09]	−0.495	4.7 [4.4]
2,6-DMPy	1.49	13.78	−0.515	9.3 [7.4]
3,5-DMPy	2.72 [2.78]	13.68 [13.40]	−0.478	6.8 [4.7]

[a] The equilibrium geometries of the monomers and their protonated forms are given in the Supporting Information. Notation: μ − dipole moment (in D); $\bar{\alpha}$ − mean polarizability (in Å^3) defined as $\bar{\alpha} = (\alpha_{11} + \alpha_{22} + \alpha_{33})/3$, where α_{ii} are the diagonal elements of the polarizability tensor; Q_N − net atomic charge (in $e-$) on N evaluated from NBO analysis (ref 39); ΔPA − relative proton affinity (in kcal/mol) defined as ΔPA = PA(msPy) − PA(Py) (the calculated and experimental proton affinities of pyridine are 221.8 and 220.8 kcal/mol (ref 41), respectively). Available experimental data are given in brackets. [b] Experimental data are from ref 40 unless indicated otherwise. [c] Experimental data are from ref 41. [d] From ref 42.

The calculations were performed with the *Gaussian 94* program package.[37]

III. Results and Discussion

A. Equilibrium Properties of Py and msPy Monomers. Before the results obtained for the water complexes are discussed, we examine some of the equilibrium properties of the isolated aromatic monomers. The B3LYP/aug-cc-pVDZ and MP2/aug-cc-pVDZ methods have been shown to provide quite similar equilibrium properties for the water monomer and the water dimer.[38] For this reason, here we analyze only the B3LYP/aug-cc-pVDZ properties of the aromatic monomers. The properties we have chosen are those which presumably determine the major part of the electrostatic and induction interaction energies, namely, the net charge associated with the N atom of the pyridine frame, the dipole moment, and the static polarizability. It should be pointed out that although we do not intend to provide very accurate predictions for these properties, in the present context it would be quite essential to reproduce the experimental trends in the Py−MPy−DMPy series. We have also calculated the proton affinity (PA) values of these molecules at the B3LYP/aug-cc-pVDZ level and compared them with available experimental data. All of these results are compiled in Table 1.

For small molecules, the B3LYP/aug-cc-pVDZ method was shown to give dipole moments which agreed with the experimental values to within 0.1 D.[43] Our results reach this level of agreement for most of the molecules in the series. The only case where the discrepancy is unusually large (0.3 D) is the 2-MPy molecule. Nevertheless, the trend in the calculated dipole moments for the entire Py−msPy series agrees well with the available experimental data.

The calculated and measured mean polarizabilities show a remarkable agreement with the exception of 4-MPy, where theory predicts a value very close to those of 2-MPy and 3-MPy, whereas the experimental value for 4-MPy is 4−5% larger than the other two. Although the averaging of the polarizability tensor elements may lead to fortuitous cancellation of errors, there are two arguments indicating that the experimental value for 4-MPy might be in error. First, in light of recent B3LYP results obtained with basis sets similar in quality to aug-cc-pVDZ[44,45] this latter discrepancy is unusually large and, second, the empirical rule of group additivity[46] is nicely reflected in the calculated $\bar{\alpha}$ values (subsequent methyl substitutions increase $\bar{\alpha}$ by about 2.1 Å^3),

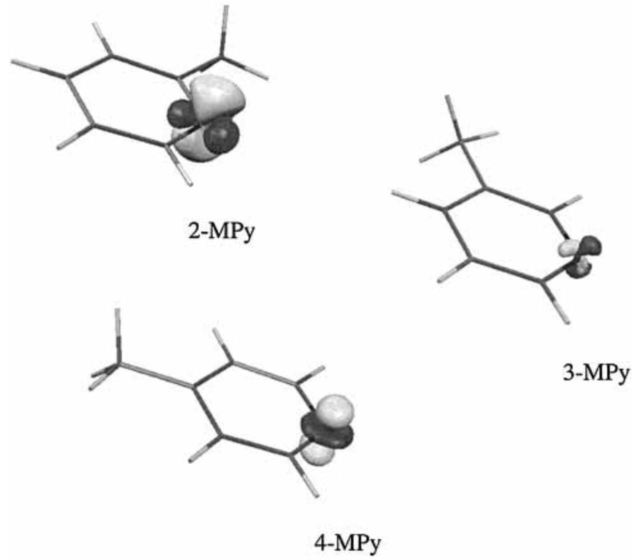

Figure 3. Change of the electron density distribution in the vicinity of N atom as a result of 2-, 3-, and 4-methyl substitution in Py. Light (dark) surfaces represent regions where the electron density is increased (decreased) upon methyl substitution. The isodensity surface is drawn at the value of 0.0005. The geometry of the Py corresponds to its equilibrium structure, and those of MPy molecules have the same C_5H_4N frame and $R(C-CH_3) = 1.51$ Å.

whereas the experimental value for 4-MPy (12.09 Å^3) does not fit with this rule.

The strength of the electrostatic intermolecular interactions in the msPy−W complexes is closely related to the electron density distribution around the N atom of the pyridine ring, which is involved as a proton acceptor in the lp···H−O and π···H−O hydrogen bonds. It is therefore interesting to analyze its variation along the msPy series.

In Figure 3, we illustrate the changes of the electron density around the N atom brought about by the 2-, 3-, and 4-methyl substitution in Py. These electron density difference plots were obtained from $\Delta\rho(r) = \rho(r)^{MPy} - \rho(r)^{Py}$, where $\rho(r)^{Py}$ and $\rho(r)^{MPy}$ are the electron densities of the Py and MPy molecules, respectively. For clarity, surfaces showing the charge reorganization around the other atoms of the pyridine frame are not shown on the plots. Note first that in line with the inductive effect of the electron donating methyl group, the magnitude of the induced changes in the charge distribution around the N atom is larger for the substitution in positions 2 (or 6) and 4 (ortho and para substitutions) than for the H/CH_3 replacement in position 3 (or 5) (meta substitution). It is also apparent that the ortho and para substitutions give rise to an increase of the electron density in the π region of the N atom, which is accompanied by a decrease of the density from the lone-pair region. These changes are consistent with the calculated net N atomic charges (Q_N) obtained from the natural bond orbital (NBO) charge partitioning scheme[39] (see Table 1). The amount of negative charge increases with respect to $Q_N = -0.488$ in Py when the methyl substitutions are at ortho and para positions ($Q_N = -0.501$ and -0.495 for 2-MPy and 4-MPy), and it shows a slight decrease in $|Q_N|$ for the meta replacements ($Q_N = -0.483$ for 3-MPy). These effects are rather small but they seem to add up in the DMPy molecules ($Q_N = -0.515$ and -0.478 for 2,6-DMPy and 3,5-DMPy, respectively).

A more characteristic measure of the proton acceptor ability of the N atom in the pyridine ring is the proton affinity. Table 1 shows that the calculated relative proton affinities (ΔPA) of the monomethylpyridines are in good agreement with experiment. They not only reproduce the absolute value of the experimental shifts from the gase-phase value of Py, but also strictly follow the experimental trend ($\Delta PA^{3-MPy} < \Delta PA^{2-MPy} < \Delta PA^{4-MPy}$) in a very narrow energy interval. The predicted shifts are somewhat larger for the two DMPy molecules, but the trend in the ΔPA values is still in line with the experimental data.

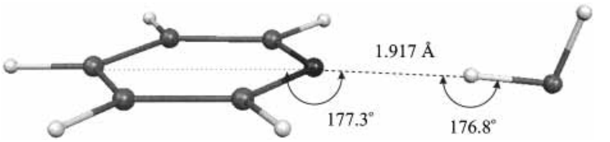

Figure 4. Equilibrium structure of the Py−W complex with selected B3LYP/aug-cc-pVDZ optimized geometrical parameters. Full geometry information for this complex is available in the Supporting Information.

It is useful to point out here that although the inductive effect of the methyl group is apparent in the proton affinities, they do not follow the variation of the Q_N values. For instance, the 3,5-DMPy molecule with its two meta-substituted CH_3 groups has the smallest amount of negative charge on N; nevertheless, its proton affinity is larger than the PA values of Py and MPy molecules. This suggests that besides the Coulombic long-range interactions higher order terms in the multipole expansion (dipole−dipole interactions, for instance) may also give important contributions to the msPy−W interaction energies.

In summary, the results presented in this section indicate that the B3LYP/aug-cc-pVDZ method is capable of reproducing the experimental trends in the selected monomer properties, therefore we expect that the electrostatic + induction part of the interaction energies in the msPy−W complexes are reasonably well reproduced at the B3LYP/aug-cc-pVDZ level.

B. The Pyridine−Water Complex. Next, we will focus on our reference system, the pyridine−water 1:1 adduct, which is known to exist in low-temperature inert matrices[47,48] and in room-temperature solutions[49−51] as well. No experimental structural data are available for this complex, but all previous calculations[21,30,52,53] suggest that the global energy minimum corresponds to the perpendicular orientation of the two molecular planes with a nearly linear N···H−O hydrogen bond. This structure is illustrated in Figure 4 along with some selected optimized geometrical parameters obtained in the present work.

The optimized intermolecular N···H bond length in Py−W is 1.917 Å, and indeed, the hydrogen bond departs only slightly from linearity ($\alpha_{CNH} = 177.3°$ and $\alpha_{NHO} = 176.8°$). The geometry of the constituent molecules is barely altered upon association. The only parameter that changes appreciably is the length of the proton donor O−H bond, which increases by 0.015 Å in the complex formation. This elongation is roughly double of that obtained by the same method for the corresponding bond in the water dimer,[38] indicating a stronger interaction in the Py−W complex. The bond length of the other OH group and the valence angle of the water molecule are essentially unaltered, and the changes in the pyridine internal parameters are very small too (less than 0.002 Å for the bond distances, and less than 0.6° for the valence angles).

The association energy of the Py−W dimer is calculated to be 6.53 and 7.68 kcal/mol at the B3LYP/aug-cc-pVDZ and MP2/aug-cc-pVDZ levels, respectively, and the corresponding BSSE corrected values are 6.08 and 6.28 kcal/mol. We note that very similar BSSE corrected association energies have been obtained by recent B3LYP and MP2 calculations (6.03 and 6.15 kcal/mol), which were carried out with a slightly smaller basis set.[21] Another recent MP2 study gave an association energy of 6.4 kcal/mol,[30] but this estimate includes only 50% of the BSSE correction.

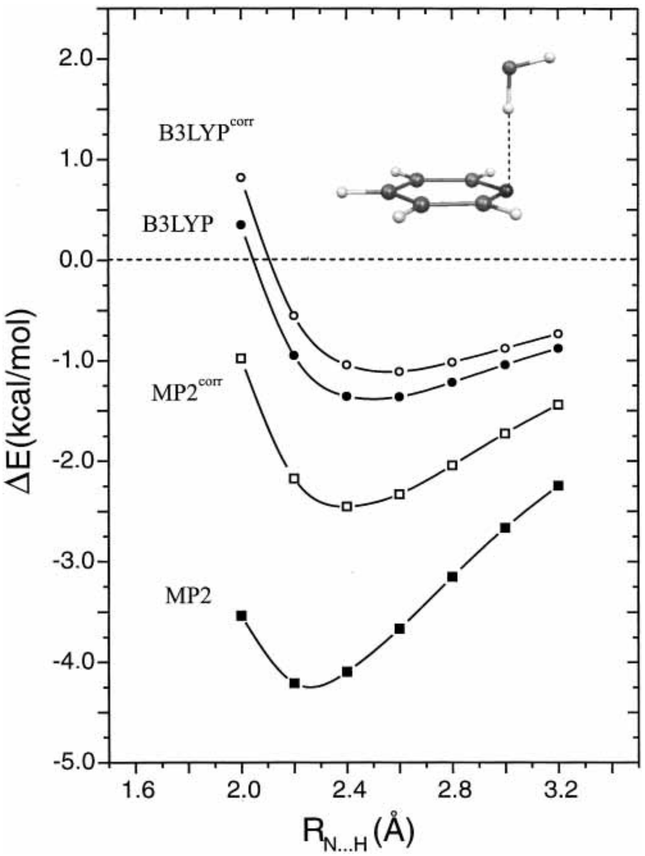

Figure 5. Py−W potential energy curves for the $\pi \cdots H-O$ type interaction, as a function of N···H distance ($R_{N\cdots H}$). The geometry of the subunits is fixed at their B3LYP/aug-cc-pVDZ equilibrium structures. The superscript “corr” denotes BSSE corrected values.

The authors of this latter work have shown that the interaction of a water molecule with the π electrons of the pyridine ring leads to considerable stabilization as well, but in contrast to the benzene−water complex, where the proton donor O−H bond points toward the center of the aromatic ring,[28,29] the $\pi \cdots H-O$ type interaction in the Py−W system is maximized when the O−H bond stands on-top of the N atom. We have also considered this type of interaction and derived potential energy curves for some of our investigated complexes. For Py−W, these single-point calculations were carried out both at the B3LYP and MP2 levels of theory. The BSSE uncorrected and corrected curves are depicted in Figure 5.

These results show quite clearly that B3LYP calculations give a significantly weaker $\pi \cdots H-O$ binding between pyridine and water, which can be attributed to the lack of dispersion interaction energy in the present DFT treatment. Although the inclusion of BSSE corrections decreases the discrepancy between the MP2 and B3LYP results (the BSSE is much smaller at the DFT level), the magnitude of the $\pi \cdots H-O$ interaction is only the half at the B3LYP level as compared to the MP2 results. The calculated MP2 interaction energy at the minimum of the BSSE corrected curve is 2.5 kcal/mol, a value which is about 40% of the interaction energy corresponding to the global minimum.

C. Methyl-Substituted Pyridine−Water Complexes. All considered msPy−W complexes exhibit energy minima for the perpendicular arrangement of their subunits similarly to what is found for Py−W (see Figure 4). The intermolecular structural parameters corresponding to the energy minima of Py−W, MPy−W, and DMPy−W complexes are given in Table 2. This table illustrates that the N···H−O bond distances in msPy−W complexes are slightly shorter than in Py−W. The α_{CNH} and α_{NHO} angles, which determine the orientation of the proton donor O−H bond relative to pyridine ring, depart from linearity to a greater extent in the 2-MPy−W and 2,6-DMPy−W complexes, indicating the steric hindrance of water coordination caused by the presence of ortho methyl groups.

TABLE 2: Intermolecular Structural Parameters of Py−W, MPy−W, and DMPy−W Complexes Obtained at the B3LYP/aug-cc-pVDZ Level[a]

	$R_{N\cdots H}$	α_{CNH}	α_{NHO}
Py−W	1.917	177.3	176.8
2-MPy−W	1.911	173.8	175.2
3-MPy−W	1.911	175.8	175.8
4-MPy−W	1.910	177.2	177.3
2,6-DMPy−W	1.915	170.7	173.2
3,5-DMPy−W	1.905	177.5	177.4

[a] Bond lengths in Å, angles in degrees.

TABLE 3: Association Energies of Py−W, MPy−W, and DMPy−W Complexes[a]

	ΔE		BSSE		ΔE_{corr}		ZPE	$\Delta E_{corr}'$	
	DFT	MP2	DFT	MP2	DFT	MP2		DFT	MP2
Py−W	6.53	7.68	0.45	1.40	6.08	6.28	1.86	4.22	4.42
2-MPy−W	6.69	8.22	0.49	1.58	6.20	6.64	1.86	4.34	4.78
3-MPy−W	6.75	7.94	0.46	1.44	6.29	6.50	1.88	4.41	4.62
4-MPy−W	6.80	7.88	0.46	1.41	6.34	6.47	1.87	4.47	4.60
2,6-DMPy−W	6.73	8.79	0.53	1.81	6.20	6.98	1.91	4.29	5.07
3,5-DMPy−W	6.91	8.14	0.45	1.46	6.46	6.68	1.85	4.61	4.83

[a] The equilibrium geometries of these complexes are given in the Supporting Information. Notation: ΔE − association energy (in kcal/mol) calculated as $\Delta E = -(E_{tot}^{msPy-W} - E_{tot}^{msPy} - E_{tot}^{W})$; BSSE − basis set superposition error; ZPE − zero point vibrational energy (both in kcal/mol); ΔE_{corr} − association energy corrected for BSSE; $\Delta E_{corr}'$ − association energy corrected for BSSE and ZPE.

Table 3 reports the calculated association energies of the investigated complexes. One of the observations that can be drawn from these results is that the association energies of msPy−W complexes are consistently larger than that of the Py−W complex. This holds true for uncorrected DFT and MP2 values (ΔE) as well as for values accounted for BSSE and ZPE corrections (ΔE_{corr} and $\Delta E_{corr}'$). The differences in ΔE (or in corrected values) between the pyridine derivatives are rather small but distinct. The B3LYP association energies are all within an energy range of 0.4 kcal/mol. On average, they gradually increase in going from Py−W to DMPy−W complexes, but they do not strictly follow the order one would expect from the proton affinities of these molecules. Figure 6, which displays the relationship between the B3LYP ΔE and PA values for the entire series, shows that the ΔE data representing the Py, 3-MPy, 4-MPy, and 3,5-DMPy molecules increase linearly as a function of PA, but those of the ortho-substituted homologues (2-MPy, 2,6-DMPy) fall well below the linear fit. This behavior is consistent with the steric effect mentioned above.

The MP2 association energies, however, seem to contradict this trend in that MP2 predicts the ortho-substituted complexes to be always more stable than the other homologues. The diagram shown in Figure 7 illustrates that the difference in the B3LYP and MP2 association energies (ΔE_{corr}) stays roughly constant (0.2 kcal/mol) along the series with the exception of the ortho-substituted complexes, where the discrepancies between the MP2 and B3LYP values are far more significant (0.44 kcal/mol for 2-MPy−W and 0.78 kcal/mol for 2,6-DMPy−W). This seeming contradiction stems again from the fact that DFT calculations do not account for dispersion interactions, which are definitely appreciable between H_2O and the methyl groups

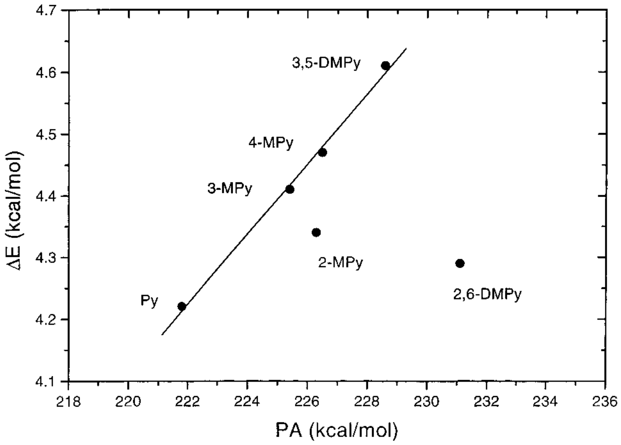

Figure 6. Correlation between B3LYP association energies (ΔE) and proton affinities (PA).

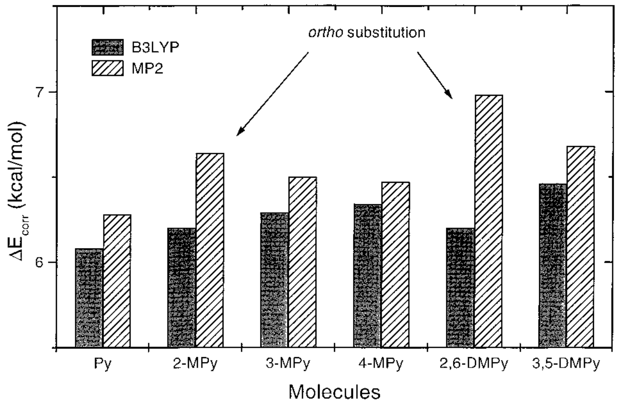

Figure 7. BSSE corrected B3LYP and MP2 association energies of msPy−W complexes.

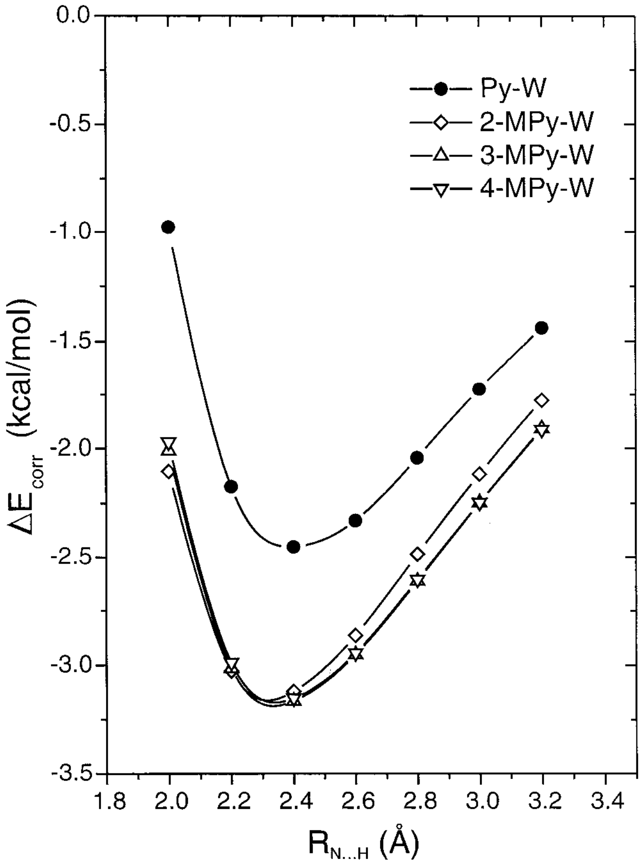

Figure 8. BSSE corrected MP2 $\pi\cdots H-O$ interaction energy curves for Py−W and MPy−W dimers, as a function of N···H distance ($R_{N\cdots H}$). The geometry and the relative arrangement of the subunits are identical to that shown in Figure 5.

in ortho positions. To verify this, we carried out MP2/aug-cc-pVDZ and B3LYP/aug-cc-pVDZ calculations for the $CH_4\cdots H_2O$ complex for an intermolecular arrangement corresponding to that of $-CH_3\cdots H_2O$ in the 2-MPy−W complex. While B3LYP calculations give practically no interaction between CH_4 and H_2O ($\Delta E_{corr} = 0.02$ kcal/mol), the BSSE corrected interaction energy at the MP2 level is 0.44 kcal/mol, which is very similar to the difference obtained between the MP2 and B3LYP association energies for 2-MPy−W. It follows then that the MP2 predictions for the relative stabilities of the msPy−W complexes are more reliable than those from B3LYP calculations.

The BSSE-corrected MP2 potential energy curves derived for the $\pi\cdots H-O$ type interaction in the monomethyl-substituted systems are compared to the corresponding Py−W curve in Figure 8. It is apparent that methyl substitution strengthens the $\pi\cdots H-O$ type interaction, but the position of the methyl group does not affect the strength of the interaction. All three MPy−W curves reach their minima at $R_{N\cdots H} \sim 2.3$ Å, where the interaction energies are 3.2 kcal/mol. This is about 0.7 kcal/mol larger than that of Py−W, which means that the stabilization induced by the methyl substitution is relatively larger for the $\pi\cdots H-O$ type bonding than for the lp···H−O interaction, where the association energies of MPy−W complexes increased only by 0.2−0.4 kcal/mol relative to that of Py−W.

D. Miscibility Behavior and Association Energies. Finally, in this section the relationship between the miscibility behavior of methyl-substituted pyridines with water and the strength of the hydrogen bond between water and pyridine molecules will be briefly discussed. It is generally agreed[1] that the necessary condition for the reappearing miscible phase is the existence of strong directional forces (e.g., hydrogen bonding interactions) between unlike molecules of the two components of the binary mixture. The majority of models[12−16] predict that the closed loop immiscibility gap becomes progressively smaller with increasing hydrogen bond strength, while a recent model[17] proposes just the opposite behavior: the extension of the immiscibility gap upon strengthening of the hydrogen bonds between water and methyl derivatives of pyridine. Thus it is of interest to compare the sequence of the hydrogen bond strengths obtained in the present paper with the experimentally observed order of the ease of miscibility with water.

Considering the lp···H−O structures, the order of methyl-substituted pyridine molecules in terms of increasing BSSE corrected MP2 association energy (ΔE_{corr}) is the following: Py < 4-MPy < 3-MPy < 2-MPy < 3,5-DMPy < 2,6-DMPy (the same order is obtained in terms of $\Delta E_{corr}'$, see Table 3), while the sequence corresponding to the ease of miscibility with water can be given as Py ≫ 4-MPy > 2-MPy > 3-MPy ≫ 2,6-DMPy > 3,5-DMPy.[2,3,10] It seems therefore that the strengthening of the hydrogen bond when going through the pyridine−monomethylpyridine−dimethylpyridine series correlates with the increasing immiscibility in the same order. On the other hand, the fine details in the solubility properties within the monomethyl and dimethyl homologues of pyridine are not reflected by the calculated association energies. This suggests that the strength of the hydrogen bonding between unlike molecules in the solution is an important, but by no means the sole parameter that determines the demixing behavior of methyl-substituted pyridines in aqueous solutions.

IV. Concluding Remarks

We have shown in this paper that although the experimental equilibrium properties of Py and msPy monomers are well reproduced at the B3LYP/aug-cc-pVDZ level of density functional theory, this method does not necessarily yield accurate hydrogen bonding interaction energies for msPy−W complexes. For meta- and para-substituted msPy−W complexes the B3LYP results match well with the MP2 predictions, but in ortho-substituted homologues, the dispersion interactions between water and the proximate CH_3 group(s) are not negligible relative to other attraction forces and the interaction energies of these systems are underestimated in the DFT treatment. The same may be said of $\pi\cdots$H−O type msPy−W interactions, for which B3LYP predicts much smaller interaction energies than MP2.

We have also shown that the association energies corresponding to the classical lone pair···H−O type hydrogen bonding in msPy−W complexes progressively increase in the Py−MPy−DMPy series, but the ordering of the calculated association energies within a given group of homologues is not consistent with the observed miscibility properties. This suggests that the differences in the miscibility behavior of the methyl-substituted pyridines cannot be simply related to the strength of the hydrogen bond that they form with the water molecule. The interaction of the apolar regions of the solute molecule with the surrounding water molecules may also play an important role in the miscibility behavior.

Acknowledgment. Hungarian Research Fund under grant OTKA T 016365 is gratefully acknowledged.

Supporting Information Available: Full geometry information for the equilibrium structure of the Py and msPy monomers, their protonated forms, Py-W and msPy-W complexes. This material is availabe free of charge via the Internet at http://pubs.acs.org.

References and Notes

(1) Narayanan, T.; Kumar, A. *Phys. Rep.* **1994**, *249*, 135.
(2) Andon, R. J. L.; Cox, J. D. *J. Chem. Soc.* **1952**, 4601.
(3) Cox, J. D. *J. Chem. Soc.* **1952**, 4606.
(4) Abe, J. I.; Nakanishi, K.; Touhara, H. *J. Chem. Thermodyn.* **1978**, *10*, 483.
(5) Marczak, W.; Giera, E. *J. Chem. Thermodyn.* **1998**, *30*, 241, and references therein.
(6) Garland, C. W.; Nishigaki, K. *J. Chem. Phys.* **1976**, *65*, 5298.
(7) Narayanan, T.; Prafulla, B. V.; Kumar, A.; Gopal, E. S. R. *Ber. Bunsen-Ges. Phys. Chem.* **1991**, *95*, 12.
(8) Schneider, G. *Z. Phys. Chem. Neue Folge* **1963**, *37*, 333.
(9) Almásy, L.; Cser, L.; Jancsó, G. *Physica B*, in press.
(10) Andon, R. J. L.; Cox, J. D.; Herington, E. F. G. *Trans. Faraday Soc.* **1957**, *53*, 410, and references therein.
(11) Hirschfelder, J. O.; Stevenson, D.; Eyring, H. *J. Chem. Phys.* **1937**, *5*, 896.
(12) Wheeler, J. C. *J. Chem. Phys.* **1975**, *62*, 433.
(13) Andersen, G. R.; Wheeler, J. C. *J. Chem. Phys.* **1978**, *69*, 3403.
(14) Goldstein, R. E.; Walker, J. S. *J. Chem. Phys.* **1983**, *78*, 1492.
(15) Walker, J. S.; Vause, C. A. *J. Chem. Phys.* **1983**, *79*, 2660.
(16) Goldstein, R. E. *J. Chem. Phys.* **1983**, *79*, 4439.
(17) (a) Brovchenko, I. V.; Oleinikova, A. V. *J. Chem. Phys.* **1997**, *106*, 7756. (b) *High Temp. High Press.* **1998**, *30*, 229.
(18) Adamo, C.; Barone, V. In *Recent Advances in Density Functional Methods*; Chong, D. P., Ed.; World Scientific: Singapore, 1997; Part II.
(19) Guo, H.; Sirois, S.; Proynov, E. I.; Salahub, D. R. In *Theoretical Treatments of Hydrogen Bonding*; Hadzi, D., Ed.; Wiley: Chichester, 1997.
(20) Lozynski, M.; Rusinska-Roszak, D.; Mack, H.-G. *J. Phys. Chem. A* **1998**, *102*, 2899.
(21) Rablen, P. R.; Lockman, J. W.; Jorgensen, W. L. *J. Phys. Chem. A* **1998**, *102*, 3782.
(22) Chandra, A. K.; Nguyen, M. T.; Zeegers-Huyskens, T. *J. Phys. Chem. A* **1998**, *102*, 6010.
(23) Mó, O.; Jáñez, M. *J. Phys. Chem. A* **1998**, *102*, 8174.
(24) Gu, J.; Leszczynski, J. *J. Phys. Chem. A* **1998**, *103*, 2744.
(25) Kristyán, S.; Pulay, P. *Chem. Phys. Lett.* **1994**, *229*, 175.
(26) Pérez-Jordá, J. M.; Becke, A. D. *Chem. Phys. Lett.* **1995**, *233*, 134.
(27) Steiner, T. *J. Chem. Soc., Chem. Commun.* **1995**, *95*.
(28) Fredericks, S. Y.; Jordan, K. D.; Zwier, T. S. *J. Phys. Chem.* **1996**, *100*, 7810.
(29) Gregory, J. K.; Clary, D. C. *Mol. Phys.* **1996**, *88*, 33.
(30) Samanta, U.; Chakrabarti, P.; Chandrasekhar, J. *J. Phys. Chem. A* **1998**, *102*, 8964.
(31) Tarakeshwar, P.; Kim, K. S.; Brutschy, B. *J. Chem. Phys.* **1999**, *110*, 8501.
(32) Kendall, R. A.; Dunning, T. H.; Harrison, R. J. *J. Chem. Phys.* **1992**, *96*, 6796.
(33) Dunning, T. H. *J. Chem. Phys.* **1989**, *90*, 1007.
(34) Becke, A. D. *J. Chem. Phys.* **1993**, *98*, 5648.
(35) Lee, C.; Yang, W.; Parr, R. G. *Phys. Rev.* **1988**, *B 37*, 785.
(36) Boys, S. F.; Bernardi, F. *Mol. Phys.* **1970**, *19*, 553.
(37) Frisch, M. J.; Trucks, G. W.; Schlegel, H. B.; Gill, P. M. W.; Johnson, B. G.; Robb, M. A.; Cheeseman, J. R.; Keith, T.; Petersson, G. A.; Montgomery, J. A.; Raghavachari, K.; Al-Laham, M. A.; Zakrzewski, V. G.; Ortiz, J. V.; Foresman, J. B.; Cioslowski, J.; Stefanov, B. B.; Nanayakkara, A.; Challacombe, M.; Peng, C. Y.; Ayala, P. Y.; Chen, W.; Wong, M. W.; Andres, J. L.; Replogle, E. S.; Gomperts, R.; Martin, R. L.; Fox, D. J.; Binkley, J. S.; Defrees, D. J.; Baker, J.; Stewart, J. P.; Head-Gordon, M.; Gonzalez, C.; Pople, J. A. *Gaussian 94*, Revision E.3; Gaussian, Inc.: Pittsburgh, PA, 1995.
(38) Kim, K.; Jordan, K. D. *J. Phys. Chem.* **1994**, *98*, 10089.
(39) Reed, A. E.; Curtiss, L. A.; Weinhold, F. *Chem. Rev.* **1988**, *88*, 899.
(40) Kozechenko, P. N.; Bulgarevich, S. B.; Movshovich, D. Ya.; Kogan, V. A.; Osipov, O. A. *Zh. Obshchei Khim.* **1982**, *52*, 670.
(41) Lias, S. G.; Liebman, J. F.; Levin, R. D. *J. Phys. Chem. Ref. Data* **1984**, *13*, 695.
(42) Sorensen, G. O.; Mahler, L.; Rastrup-Andersen, N. *J. Mol. Struct.* **1974**, *20*, 119.
(43) Wang, J.; Johnson, B. G.; Boyd, R. J.; Eriksson, L. A. *J. Phys. Chem.* **1996**, *100*, 6317.
(44) Ioannou, A. G.; Colwell, S. M.; Amos, R. D. *Chem. Phys. Lett.* **1997**, *278*, 278.
(45) Cohen, A. J.; Tantirungrotechai, Y. *Chem. Phys. Lett.* **1999**, *299*, 465.
(46) As an example for the additivity of polarizability of the methyl group, see: Aue, D. H.; Webb, H. M.; Bowers, M. T. *J. Am. Chem. Soc.* **1976**, *98*, 311.
(47) Maes, G. *Bull. Soc. Chim. Belg.* **1981**, *90*, 1093.
(48) Maes, G.; Smets, J. *J. Mol. Struct.* **1992**, *270*, 141.
(49) Takahashi, H.; Mamola, K.; Plyler, E. K. *J. Mol. Spectrosc.* **1966**, *21*, 217.
(50) Kasende, O.; Zeegers-Huyskens, Th. *Spectrosc. Lett.* **1980**, *13*, 493.
(51) Zoidis, E.; Yarwood, J.; Danten, Y.; Besnard, M. *Mol. Phys.* **1995**, *85*, 373. Zoidis, E.; Yarwood, J.; Danten, Y.; Besnard, M. *Mol. Phys.* **1995**, *85*, 385.
(52) Del Bene, J. E. *J. Am. Chem. Soc.* **1975**, *97*, 5330.
(53) Alagona, G.; Ghio, C.; Nagy, P. *J. Mol. Struct. (THEOCHEM)* **1989**, *187*, 219.